

RIJKSUNIVERSITEIT GRONINGEN

BACHELOR THESIS

---

Thickness of the gaseous discs of  
galaxies at  $z > 4$

---



**rijksuniversiteit  
 groningen**

*Author:*  
Berber Schuurman

*Supervisors:*  
Filippo Fraternali  
Fernanda Roman de Oliveira  
Francesca Rizzo

### Abstract

Measuring the thickness of galaxy discs is a difficult task. The thickness is therefore often neglected or arbitrarily assumed, however it does have an effect on the geometric and kinematic measurements of galaxy discs. Studying disc thickness throughout cosmic time is crucial to understand disc formation. In this work, we investigate the thickness of the gaseous disc of a hydro-dynamical cosmological simulated galaxy 'Petunia' at  $z = 7$  using mock [CII] emission-line datacubes. This thesis builds upon former research done by [Roman-Oliveira et al. \[2023\]](#), that presents CANNUBI, a tool to estimate geometric parameters, to derive the thickness of galaxy discs. The aim is to test the reliability of CANNUBI by using it on simulated galaxy Petunia. First, we estimate the thickness from an idealised edge-on view of the simulated galaxy, which we take as the true thickness of Petunia. Secondly, we measure the thicknesses and inclination on the mock [CII] emission-line datacubes at inclinations:  $30^\circ$ ,  $60^\circ$  and  $80^\circ$ . Lastly, we investigate the recovery of the thickness and inclination with the true values. The results are as follows: i) We find that the thickness of Petunia is roughly constant along its radial extent, with a median thickness of  $0.065^{+0.002}_{-0.009}$  kpc. ii) CANNUBI was able to recover the thickness and inclination of the discs within the  $1\sigma$  error, except for the  $80^\circ$  inclination mock data. The tests support the thickness measurements in [Roman-Oliveira et al. \[2023\]](#), where they found thicknesses of the order of 1 kpc for 5 galaxies at  $z = 4.5$ .

## Acknowledgements

First and foremost, I would like to express my gratitude to my supervisors, Filippo Fraternali, Fernanda Roman de Oliveira and Francesca Rizzo, for their guidance and support throughout this project. Thank you for sharing your research on this interesting topic and for taking the time to assist me. Your efforts have greatly contributed to this thesis.

Secondly, I would like to thank my fellow students and friends, Annemarijn Zwerver and Abel Kersten. They have been a huge support to me.

Lastly, I would like to acknowledge the creators of the hydro dynamical cosmological **SERRA** simulation suite [[Pallottini et al., 2022](#)] and [Rizzo et al. \[2022\]](#) for providing the data on simulated galaxy Petunia.

## Contents

<b>1</b>	<b>Introduction</b>	<b>5</b>
1.1	Disc thickness in nearby galaxies . . . . .	5
1.2	Disc thickness in high-redshift galaxies . . . . .	7
1.3	Motivation . . . . .	8
1.4	This thesis . . . . .	9
<b>2</b>	<b>Data</b>	<b>10</b>
2.1	Mock galaxies, generated with GALMOD . . . . .	10
2.2	Petunia, a galaxy from the SERRA simulation . . . . .	11
2.3	From SERRA simulation to datacube . . . . .	12
<b>3</b>	<b>Methodology</b>	<b>13</b>
3.1	Thickness estimation . . . . .	13
3.2	CANNUBI . . . . .	16
3.2.1	Python script: CANNUBI . . . . .	16
3.2.2	Parameters in CANNUBI . . . . .	17
3.2.3	CANNUBI on idealised galaxy models . . . . .	18
<b>4</b>	<b>Results and Discussion</b>	<b>20</b>
4.1	True thickness of Petunia . . . . .	20
4.2	CANNUBI on the simulated galaxy Petunia . . . . .	21
4.2.1	Flux maps . . . . .	21
4.2.2	Recovered inclination and thickness . . . . .	22
4.3	Reliability . . . . .	25
4.4	Implications . . . . .	25
<b>5</b>	<b>Conclusions</b>	<b>26</b>
	<b>Appendix A</b>	<b>30</b>
	<b>Appendix B</b>	<b>31</b>

# 1 Introduction

Galaxies come in a fascinating variety of shapes and sizes. From the Sloan Digital Sky Survey we know that in the local Universe, around 85% of galaxies contain a disc [York and et al., 2000]. Galaxy discs form through gas accretion from the environment towards the centre of dark matter halos [e.g. Fall and Efstathiou, 1980]. The conservation of angular momentum of the infalling gas leads to a rotationally supported gaseous disc in which star formation takes place. Despite rotation being the dominant motion of galaxy discs, random motions are always present in both the stellar and the gaseous component. Such random motions make the discs thickness non-negligible. In the case of the gas component, the random motions are both thermal and due to the presence of turbulence, which is often the dominating effect. The thickness of the gaseous discs of galaxies is then the outcome of the interplay between gas turbulence and gravity and it is tightly linked to both star formation and the energy release via supernova explosions [e.g. Krumholz et al., 2018, Bacchini et al., 2020].

The past research on the thickness of galaxy discs has been almost exclusively done on nearby galaxies [e.g. Bacchini et al., 2019]. However, studying the thickness of discs of high- $z$  galaxies can give us insights on how galaxy discs form and evolve through cosmic time. The gaseous discs of the galaxies in the Early Universe are the sites of early star formation and thus the birth places of the old stellar population of present-day galaxies. Therefore, the thickness of early gaseous discs contain information about the formation of present-day stellar thick discs and the build up of baryonic mass in galaxies. The two main theories on the formation of thick disks are: 1) Stars were originated in the thin disc and moved to the thick disc. 2) In the Early Universe stars started to form in thick discs and in the Late Universe began to form in thin discs [van der Kruit and Freeman, 2011]. In addition to providing insights in disc formation, taking into account the thickness of galaxy discs, currently often neglected, can have important effects on the derivation of the kinematic and dynamical properties of a galaxy [e.g. Mancera Piña et al., 2022]. Thus, improving and deriving robust techniques to measure the thickness of discs can enhance the reliability of kinematic studies across cosmic time.

## 1.1 Disc thickness in nearby galaxies

Galaxies discs are made up of gas and stars. The stellar component of nearby galaxies like our Milky Way are typically made out of a thin disc and a thick disc [e.g. Kuijken and Gilmore, 1989]. In Figure 1 we show the thin disc in the lower panel and the thick disc in the upper panel in nearby galaxy, NGC 4565. Stars in the thin disc are younger, more metal rich and closer to the vertical midplane compared to the older, metal poor, stellar populations found in the thick disc. The average vertical dispersion of thick disc stars is larger than that of thin disc stars, allowing them to reach higher distances above and below the midplane of the disc [Yoachim and Dalcanton, 2006].

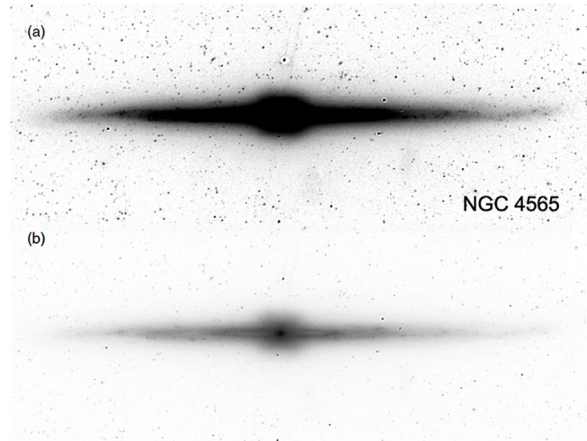


Figure 1: Edge-on image of NGC4565 observed with Spitzer/IRAC  $3.6 \mu\text{m}$ . Both panels show the same image with different contrast so it highlights the structure of the thick disc (top panel) and the thin disc (bottom panel) [Kormendy and Bender, 2019].

The Milky Way disc is an optimal laboratory to study the detailed distributions of gas and stars along the radial and vertical direction, allowing the reconstruction of the 3D distribution and kinematics of stellar populations of different ages across thin and thick discs. Moreover, the Galactic interstellar medium (ISM) is also known in great details. The gaseous component of the disc, the ISM, is mostly made of hydrogen: neutral atomic (HI), ionised (HII) and molecular ( $\text{H}_2$ ). The second most abundant element is helium (He) but also metals are critically important for the chemistry and the physics of the ISM. To study the different components we need to observe them through different tracers. HI is often observed through the 21 cm line, HII can be observed through the recombination lines or forbidden lines of ionised species such as oxygen ([OII], [OIII]).  $\text{H}_2$ , on the other hand, is notoriously difficult to observe directly and needs to be probed by a proxy such as the CO molecule [Sparke and Gallagher, 2007].

A number of studies of the vertical structure of the ISM in the Milky Way have shown that the various gas components have different thicknesses, with the "colder" components, such as molecular gas, being thinner than the "warmer" components such as the ionised gas (e.g. Bacchini et al., 2020). Moreover, the thickness is not constant but instead it increases with radius. This effect is called flaring of the gaseous disc and it is also observed in external galaxies. The physical phenomenon that explains the disc flaring is hydrostatic equilibrium where the gas pressure, thermal and turbulent motions, counteract the gravitational pull. In the outskirts of the disc, the gravitational pull is weaker and the scale height increases. The gravitational force is due to the stars, the dark matter and to the self-gravity of the gas. The pressure force of the ISM components varies mainly based on their distinct temperatures and turbulence, leading to differences in their thicknesses.

In a recent paper by Bacchini et al. [2019], the HI disc scale height was derived using the assumption of hydrostatic equilibrium. The disc scale height varies from less than 100 pc in the inner regions to  $\sim 0.8$  kpc in the outskirts of the Milky Way disc. Figure 2 shows such thickness and compares it with the measured thickness of young stars, traced by classical Cepheids. The fact that the two perfectly overlap indicate that stars are currently forming with the same vertical distribution of the gas and confirms the importance of determining the thickness of gaseous galaxy discs.

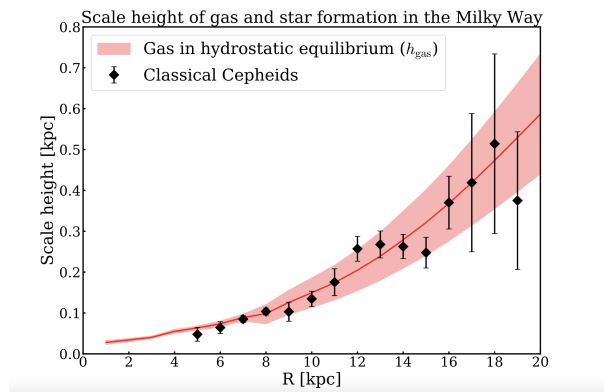


Figure 2: The radial profile of the disc scale height of the Milky Way. The measured scale height of young stars is shown with black points while the gas scale height inferred through hydrostatic equilibrium is shown in red. Figure from [Bacchini et al. \[2019\]](#).

## 1.2 Disc thickness in high-redshift galaxies

The research on thickness of galaxy discs at high-redshift is relatively new and rapidly developing. In the past years, significant advancements in observational capabilities have allowed telescopes like ALMA (Atacama Large Millimeter/submillimeter Array) and the James Webb Space Telescope to provide us with more detailed observations of the Early Universe. With these advanced telescopes, researchers have been able to detect disc galaxies at least up to  $z \sim 5$  [e.g. [Rizzo et al., 2020](#), [Roman-Oliveira et al., 2023](#), [Robertson et al., 2023](#)]. The velocity dispersion, which provides a direct measure of random motion, is found to be relatively high in high-redshift discs compared to local galaxies, suggesting the presence of thick disc structures [[Weiner et al., 2006](#)].

Measuring the thickness and velocity dispersion of galaxies at high- $z$  is, however, very challenging, due to the cosmic evolution of the angular diameter distances, the intrinsic evolution of the galaxy sizes and the cosmological dimming. Accurate measurements of the velocity dispersion require, instead, spatially resolved observations [e.g. [Rizzo et al., 2022](#)]. Having fewer independent resolution elements covering the emission of a galaxy severely limits the robust recovery of kinematic properties. This is mainly due to the beam smearing effect which can blend the line-of-sight signatures of rotation velocity and velocity dispersion due to poor spatial resolution [[Bosma, 1978](#)]. If not properly accounted for, beam smearing can cause the overestimation of velocity dispersion and the underestimation of rotation velocity in each observed beam.

In the high- $z$  Universe we also do not have access to kinematic tracers commonly used in the local Universe such as HI. At  $z > 4$ , the [CII]  $158 \mu\text{m}$  is the best tracer for the cold gas distribution and it is a useful tool to tackle the limitations discussed above. The [CII] emission-line is emitted by galaxies at  $z > 4$  and is redshifted and observable in the range of 0.8 and 1.3 mm, which is covered by ALMA. Moreover, the [CII] emission-line traces multiple phases of the ISM, from molecular to ionised gas, which makes it the most extended emission-line and an optimal kinematic tracer [[Carilli and Walter, 2013](#)]. Additionally, it stands out as one of the brightest emission-lines.

In a study by [Walter et al. \[2022\]](#), an attempt was made to estimate the gaseous disc thick-

ness of a quasar at  $z = 6.9$  observed with ALMA. The thickness of the quasar has been derived by measuring the gas velocity dispersion and assuming hydrostatic equilibrium, which yielded an estimate in the range of a relatively thin disc ( $\sim 0.1$  kpc) all the way up to a relatively thick disc ( $\sim 1$  kpc). Given that this disc extends for about 2.6 kpc in radius, the large uncertainty on the disc thickness has a significant impact on our ability to interpret the results.

### 1.3 Motivation

In this project, we investigate the thickness of the gas disc of a simulated galaxy at  $z = 7$  using mock [CII] emission-line datacubes. We will examine their geometrical properties with focus on thickness and inclination. This study builds upon former research done by [Roman-Oliveira et al. \[2023\]](#). The results could potentially lead to new knowledge about the formation of thick discs.

In their recent study, [Roman-Oliveira et al. \[2023\]](#) measured regular rotation and low turbulence in a diverse sample of galaxies, they used high spatial resolution data of the [CII] emission-line of 5 galaxies at  $z \sim 4.5$ . The flux map and velocity field is shown for one of these galaxies, BRI1335-0417, in Figure 3. Their analysis suggests that the galaxies in their sample display high levels of rotation support. The aim of this thesis is to validate their results on the thickness of the galaxy discs. The latter are derived using CANNUBI, a tool which fits the geometric parameters of the galaxies (e.g. inclination angle, centre).

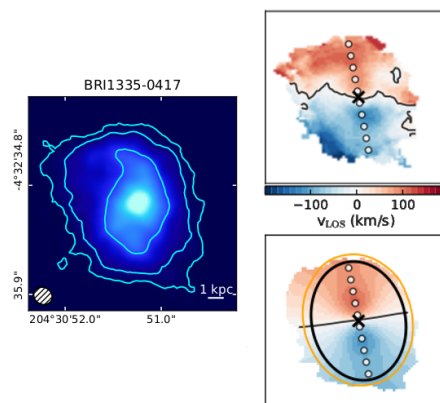


Figure 3: The results from [Roman-Oliveira et al. \[2023\]](#) on galaxy: BRI1335-0417. Left panel: The total flux map. Right panel: The velocity field observed on the top and the obtained model on the bottom.

The galaxies studied in [Roman-Oliveira et al. \[2023\]](#) have inclinations of  $\sim 42^\circ$ , a value lower than an inclination of  $60^\circ$  expected for a sample of galaxies randomly oriented galaxies [[Romanowsky and Fall, 2012](#)]. One possible explanation could be a systematic underestimation of the inclination due to the assumption of a razor thin disc, which also impacts the derived kinematic properties of the discs. If the assumption of a razor thin disc is relaxed, and the thickness is let free to vary, CANNUBI finds thickness of the galaxies of  $\sim 1$  kpc.

In [Roman-Oliveira et al. \[2023\]](#), the reliability of CANNUBI is tested using 49 ALMA mock observations of idealised galaxies generated using GALMOD within the <sup>3D</sup>BAROLO tool [[Di Teodoro and Fraternali, 2015](#)]. The mocks included galaxies with inclinations between  $30^\circ$  and  $70^\circ$  and thicknesses between 0 and 1.6 kpc. The true inclinations and thicknesses are on average recovered by



CANNUBI within  $1\sigma$ . However, being regularly rotating, smooth and axisymmetric, the galaxies used for such tests may be unrealistic. To further assess the reliability of CANNUBI to measure the disc thickness, it is necessary to test it with more realistic mock data, such as with galaxies from hydrodynamical cosmological simulations.

#### 1.4 This thesis

The structure of this thesis is as follows: In Chapter 2, we describe the data used to validate CANNUBI. In Chapter 3, we present the assumptions and methods used to measure the thickness of a simulated galaxy and the mock data. In Chapter 4 the true values and the CANNUBI recovered values for the inclination and thickness are presented and discussed. Chapter 5 contains the implication of our results and the conclusion.

## 2 Data

The aim of this research is to understand whether the thickness and inclination of high- $z$  galaxies can be recovered using state-of-the-art observations and tools. `CANNUBI` is a python script designed to infer geometrical properties of rotating disc galaxies using 3D modelling of emission-line datacubes with a Markov Chain Monte Carlo approach <sup>1</sup>. In particular, `CANNUBI` is designed to provide accurate estimates of the inclination and thickness of the disc. To validate its results we examine mock data from hydro-dynamical simulations, where, in principle, the true values of these parameters can be known. Before doing that we examine three idealised models, which are rather simplistic representations of galaxies. Then, we will examine the simulated galaxy: Petunia, from the SERRA cosmological simulation suite [Pallottini et al., 2022]. We run `CANNUBI` on mock data produced from this simulation and compare the results with the true thickness and inclination. The true value of the thickness of Petunia is not known in this case, thus we designed a method to estimate it robustly which will be covered in this section.

### 2.1 Mock galaxies, generated with GALMOD

In this study, the mock data are in the form of an emission-line datacubes. A datacube is a three-dimensional array consisting of a two-dimensional spatial axes and a spectral (velocity) axis. A datacube records the flux of a certain emission line at various positions (along the line of sight) across the galaxy disc. It does so by collecting the flux per range of velocities, called channel maps. The Doppler effect spreads the emission across the various channels. By studying this cube, it becomes possible to have a deep understanding of the kinematics and distribution of the gas in the galaxy. Summing all the channel maps or integrating all the line profiles across the whole field of view yields the total flux map of the specific emission line.

We first examine the behaviour of `CANNUBI` for three axisymmetric and idealised mock galaxies with different geometrical properties. The mock galaxies are generated with `GALMOD` within `3D BAROLO` [Di Teodoro and Fraternali, 2015]. `3D BAROLO` creates a mock emission-line cube of a disc galaxy using the so-called tilted ring model, which represents galaxies as a finite number of rings with different kinematic and geometric properties. The geometrical parameters of the rings are inclination angle (`INC`), centre ( $x_0, y_0$ ), thickness (`Z0`) and position angle (`PA`), they are often assumed constant with radius. The motion of the gas is described per ring, in particular its rotation ( $v_{rot}$ ) and velocity dispersion ( $v_{disp}$ ). Random noise is added to the entire datacube and it is then convolved with a Gaussian kernel to simulate a limited angular resolution of real observations.

The true values for the thickness and the recovered ones from `CANNUBI` will be compared and conclusions can be drawn about the achieved accuracy. Here we consider three models selected from a series specifically produced to test the performance of `CANNUBI`. Model 1 has a thickness of  $10''$  and an inclination of  $30^\circ$ , model 2 has a thickness of  $10''$  and inclination of  $66^\circ$  and model 3 has a thickness of  $85''$  and inclination of  $75^\circ$ . Furthermore, these models have a high spatial resolution with a beamsize of  $55''$  relative to a disc with a radial extent of roughly  $600''$ . Model 3 is an example of a galaxy with an exceptionally thick disc.

---

<sup>1</sup>Available at <https://www.filippofraternali.com/cannubi>.

## 2.2 Petunia, a galaxy from the SERRA simulation

The mock galaxies in Section 2.1 are idealised representations where the gas distribution is perfectly axisymmetric, the discs are fully co-planer and the gas is in circular motions. However, this is not the case for most galaxies. To properly test the reliability of CANNUBI on more realistic galaxies, we used ALMA mock data obtained from hydro-dynamical cosmological simulation, SERRA. The SERRA sample includes 202 galaxies at  $z > 6$  with masses ranging  $10^7 M_\odot \lesssim M_* \lesssim 10^{10} M_\odot$  [Pallottini et al., 2022]. For this work, we choose to inspect the disc structure of the galaxy Petunia, which has a well behaved, rationally supported gas disc. Petunia is a galaxy at  $z = 7.0$  with a mass of  $1.8 \times 10^{10} M_\odot$ . Given the cosmology of Planck Collaboration [2020], the physical scale at this redshift is  $1078 Mpc$ .

We use emission-line datacubes with a disc inclination of  $30^\circ$ ,  $60^\circ$  and  $80^\circ$ , which have an angular resolution of  $0.02''$ . Furthermore, to test the possible effects of data quality we use another mock datacube with an inclination of  $60^\circ$  and an angular resolution of  $0.05''$ . For comparison, the diameter of the galaxy disc is about  $0.30''$ . In Figure 4, we display the total flux maps with the two different resolutions on the three inclinations. These cubes have signal-to-noise ratio (S/N) of 10 [Rizzo et al., 2022]. For visualisation purpose, the centre  $((x_0, y_0) = (0, 0))$  is defined as the brightest value of Petunia at an  $80^\circ$  inclination for all figures.

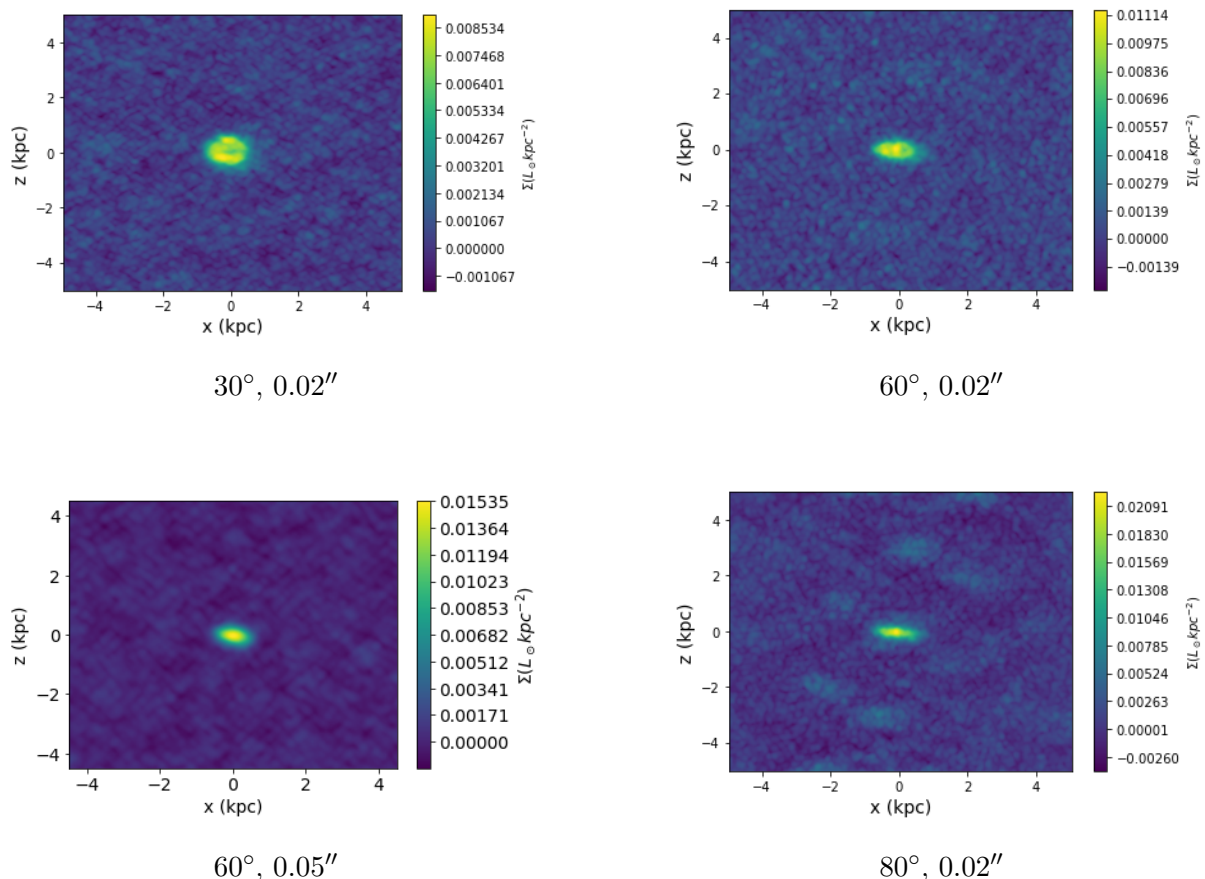


Figure 4: Total flux maps of the ALMA [CII] mock data for Petunia. The inclination and resolution is shown below each panel. The colorbar indicates the surface brightness in  $L_\odot kpc^{-2}$ .

### 2.3 From SERRA simulation to datacube

In this Section, we will provide a brief overview of how the mock data used in this study were obtained from the SERRA simulation. This mock data imitates how we observe galaxies through a telescope in real life. ALMA observes the galaxies by targeting the [CII] 158  $\mu m$  emission-line. In the SERRA simulation galaxies form following the standard cosmological model that starts of from predefined initial conditions at  $z = 100$ . The SERRA suite uses a grid-based code producing a cubic box containing a number of cells. These cells have three position and three velocity components, which contain properties of the gas such as temperature and density. The abundances of [CII] and the line-emission is computed using a spectral synthesis code, CLOUDY, as outlined in Kohandel et al. [2020]. The 6D simulation box is then projected along the line-of-sight to simulate an observation and produce a 3D mock datacube of the [CII] emission-line with two spatial axes and one velocity axis. The last step to come closer to actual ALMA observations is to imitate the observational limitations such as noise and a convolution matching the resolution of typical real data. This has been done using the task SIMOBS within CASA and the details are described in [Rizzo et al., 2022].

### 3 Methodology

#### 3.1 Thickness estimation

Our main goal is to compare the recovered thickness of the simulated galaxy Petunia from CANNUBI with the true value known a priori. The available thickness estimation determined by the SERRA team is not usable in the context of this research. They measured the value for the thickness considering only a specific region of the galaxy within a certain gas density range. Therefore, we used an alternative approach to determine a thickness value based on an easily manageable emission-line datacube of Petunia: an edge-on view of the disc with no noise. We extracted the thickness using the total flux map of this cube.

In Figure 5 on the left panel, we show the total flux map obtained from the edge-on view datacube of Petunia. The disc is located in the central region with a position angle of about  $90^\circ$  (bright yellow emission). Streams and cloud-like structures are visible surrounding the galaxy disc. The disc contains the majority of the mass, therefore it dominates the surface brightness. However, this galaxy is actively forming stars and going through gas accretion events which show up as low level emission structures around the galaxy. In this study, we will refer to these structures as diffuse emission. The dark colored region of the image is the background and has a non-zero constant value (see lowest value color bar in Fig. 5). In the right panel of Figure 5, we show a zoomed on the disc of Petunia, which points out to the existence of a small warp in the outer disc (red arrows).

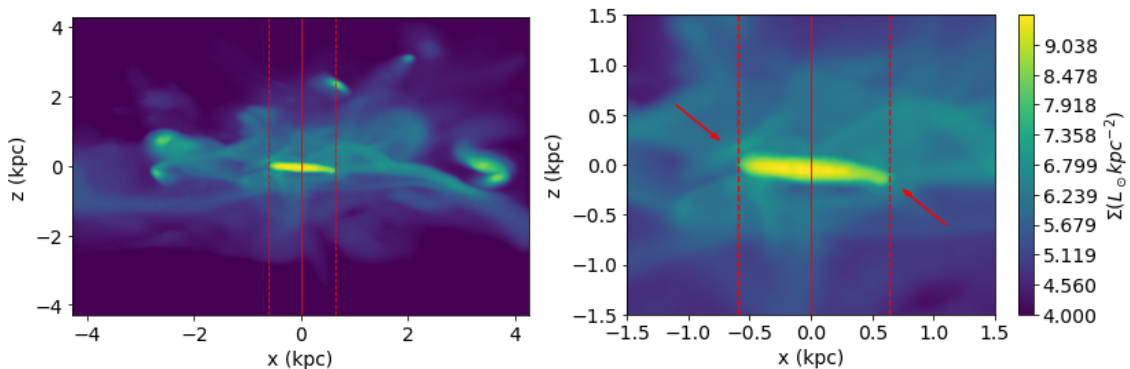


Figure 5: This figure shows the edge-on view of the mock data obtained from the simulated galaxy Petunia. Left panel: The solid line is the centre of the disc and the dashed lines indicate the two edges. Right panel: The total flux map zoomed in on the galaxy disc. The colorbar shows the surface brightness in  $L_{\odot} \text{kpc}^{-2}$ , for the left panel as well. The red arrows point out Petunia’s warp.

In this analysis, we focus only on the vertical surface brightness distribution (e. g. along the direction visualized as the red lines in Figure 5, which is extracted perpendicular to the disc since Petunia has a PA of around  $90^\circ$ ). It is this profile that can be used to obtain the thickness of the galaxy disc. The surface brightness data were extracted along vertical stripes of pixels with width of one pixel from the total flux map (e.g. red lines in Figure 5). This was done only over the horizontal extent of the disc, indicated by the dashed red lines. The disc spans a total size of  $1.2 \text{kpc}$  from  $-0.6 \text{kpc}$  to  $+0.6 \text{kpc}$ .

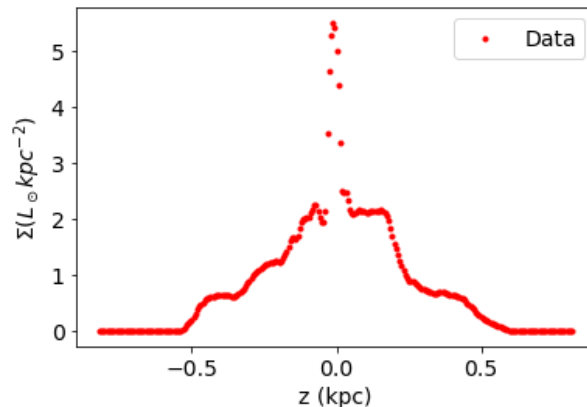


Figure 6: The data along the solid red line of Figure 5, for which the background has been subtracted. The disc and diffuse emission component are clearly visible.

Through this approach, we get one vertical distribution per pixel, one of which is shown in Figure 6. From the Figure it is clear that the emission from Petunia consists of two components, a narrow component tracing the disc and a larger component tracing the diffuse emission. To model this emission, we assume a vertical density and an exponential profile for the narrow and broad components, respectively. In practice, we aim to reliably describe the narrow peak by eliminating the contribution of the diffuse emission. The detailed behaviour of the diffuse emission is not our focus and we have found that an exponential profile describes it well in most cases.

In the literature, both Gaussian- and  $sech^2$ -functions are used to describe vertical density profiles of galaxy discs [e.g. [Koyama and Ostriker, 2009](#), [van der Kruit and Searle, 1981](#)]. These equations are based on the assumption of hydrostatic equilibrium in two different types of gravitational potentials and on local thermal equilibrium. By using one of the other formulation, our final model is therefore defined by the following equations for the surface brightness ( $\Sigma$ ) of the gas as a function of height ( $z$ ):

$$\Sigma(z) = \Sigma_{0,1} sech^2\left(\frac{|z - z_0|}{h_1}\right) + \Sigma_{0,2} e^{-\frac{|z - z_0|}{h_2}}, \quad (1)$$

$$\Sigma(z) = \Sigma_{0,1} e^{-\frac{(z - z_0)^2}{2h_1^2}} + \Sigma_{0,2} e^{-\frac{|z - z_0|}{h_2}}, \quad (2)$$

where  $\Sigma_{0,1}$ ,  $\Sigma_{0,2}$  are the central brightness's,  $h_1$ ,  $h_2$  are the scale heights and the midplane is located at  $z_0$ . Note that the absolute value in the  $sech^2$ - and exponential functions are taken so that the emission can be fitted in the plus- and minus-direction (relative to the mid plane).

We use Equations 1 and 2 to fit the vertical distribution of Petunia in the pixel range that covers the main disc structure as shown in Figure 5. To find the best-fit parameters that define equations 1 and 2 we perform the fitting using the least square optimisation algorithm `CURVE FIT` as implemented in `SCIPY` library [[Virtanen et al., 2020](#)]. The final scale height,  $h$ , is determined by the best fit.

To give insights on the goodness of the fit, we computed the coefficient of determination,  $R^2$ , defined as:

$$R^2 = \frac{\sum_i (\Sigma_i - \hat{\Sigma}_i)^2}{\sum_i (\Sigma_i - \bar{\Sigma})^2}, \quad (3)$$

where  $\Sigma_i$  is the observed surface brightness,  $\hat{\Sigma}_i$  is the surface brightness of the model and  $\bar{\Sigma}$  the mean of the observed values.  $R^2$  estimates the goodness of the fit, where a value of 1 indicates a perfect fit. In Figure 7, the  $R^2$  values of the fits are plotted as a function of radius for both functions.

The mean values of  $R^2$  are 0.95 and 0.94 for the Gaussian and  $sech^2$  functions, respectively. This tells us both functions are a good description of the data. For the rest of the Chapter, we decided to focus on the values of the parameters derived from the Gaussian function. We note that our conclusions do not change if the parameters obtained from the  $sech^2$  functions are considered.

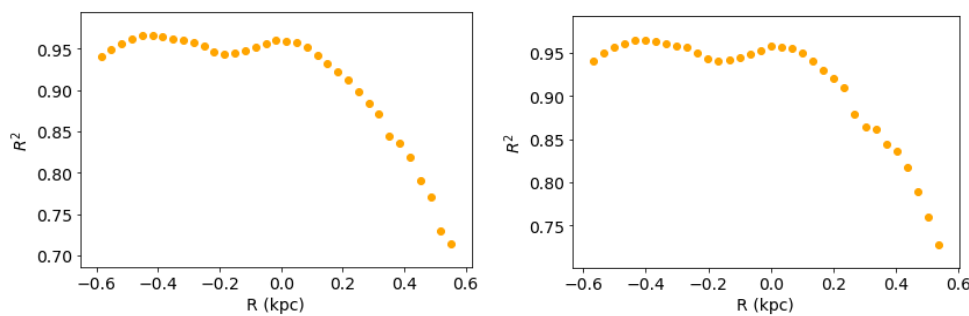


Figure 7:  $R^2$  of the fits a function of radius for the two different models across the radial extent across the disc of Petunia. On the left panel, we show the Gaussian fit and on the right panel we show the  $sech^2$  fit.

As a result of our fitting, we obtained the best-fit parameters defining Eq. 2 (i.e.,  $\Sigma_{0,1}$ ,  $z_0$ ,  $h_1$ ,  $\Sigma_{0,2}$ ,  $h_2$ ) and their uncertainties, where  $h_1$  is the final disc thickness to be compared with  $Z_0$  from CANNUBI.

In Figure 8, the red circles show the vertical surface brightness profiles extracted from the centre ( $R = 0$  kpc, left panel) and the edge of the disc ( $R = 0.6$  kpc, right panel). In the same Figure, we show the best-fit models (solid orange line) and the two components defining the disc and diffuse emission (dotted blue and dashed green). The right panel is an example of a bad fit, where the narrow component is not well fitted by the Gaussian function due the strong contamination by the diffuse emission. In this case, the value of  $R^2$  is 0.72. All fits with  $R^2 < 0.9$  fits are removed from the results.

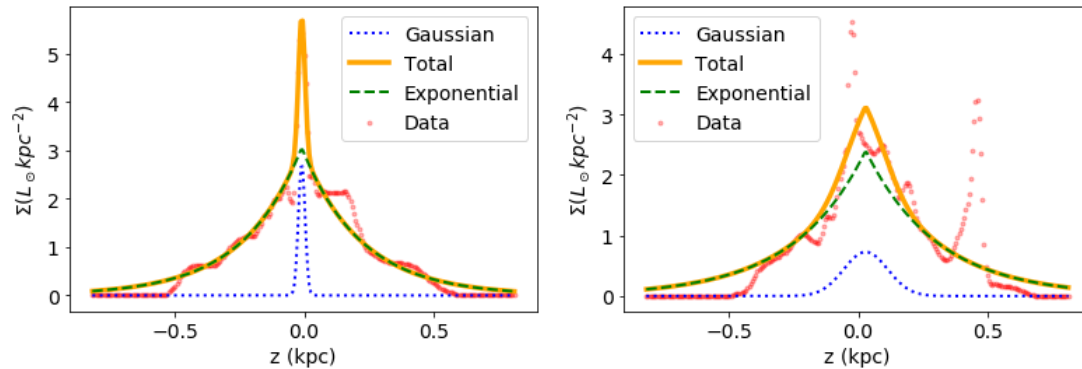


Figure 8: Vertical surface brightness profiles of Petunia edge-on (red circles). The orange solid line shows the model, obtained as the sum of the exponential (green dashed) and Gaussian (blue dotted) profiles. Left: Vertical profile in the inner region ( $R = 0$  kpc). Right: Vertical profile at the edge of the disc ( $R = 0.6$  kpc).

To compute a unique value of the thickness for Petunia, we considered the median values of the distribution of the disc thickness,  $h$ , from the pixels in which  $R^2 \geq 0.9$ . The uncertainty in the  $h$  distribution is computed by subtracting the 16th and 84th percentile from the 50th percentile, which yields the  $1\sigma$  uncertainty. We also account for the individual uncertainties by summing their mean with the  $1\sigma$  uncertainty in quadrature, following error propagation analysis.

## 3.2 CANNUBI

### 3.2.1 Python script: CANNUBI

CANNUBI is a tool to estimate geometrical parameters of a rotating galaxy disc from emission-line datacubes [Roman-Oliveira et al., 2023]. It uses <sup>3D</sup>BAROLO, a software designed to fit a 3D tilted-ring model to the emission-line data of a galaxy [Di Teodoro and Fraternali, 2015]. The main purpose of CANNUBI is to fix the geometrical parameters of the disc when performing the kinematic fit with <sup>3D</sup>BAROLO, thus considerably reducing the number of free parameters.

The determination of the geometrical parameters can greatly affect the interpretation of the kinematics of rotating discs. A key source of uncertainty is related to determining the inclination of a disc which is used to turn the line-of-sight velocity into the rotation velocity. To determine the inclination of a galaxy disc it is often assumed that the disc is razor thin and therefore the inclination (INC) is simply given as:

$$INC = \cos^{-1} \frac{A}{B}, \quad (4)$$

where INC is the inclination and A and B are the major and minor axis, respectively. However, real galaxy discs are not razor thin but have a finite thickness that can be non-negligible in some cases, especially in high- $z$  galaxies. It is easy to see that a thick disc seen in projection along the line of sight at a relatively high inclination can have an appearance similar to a razor-thin disc with low inclination (Fig. 9), i.e. inclination and thickness are degenerate. From Eq. 4 and Figure 9 it becomes clear that the assumption of a razor thin disc maximises the  $A/B$  ratio which in turn leads to an underestimation of the inclination.





Figure 9: Left panel: Thick disc ( $Z_0 > 0$ ) seen at  $\sim 60^\circ$  inclination. Right panel: Thin disc ( $Z_0 = 0$ ) seen at  $\sim 60^\circ$ .

CANNUBI uses the EMCEE Python package to perform Markov Chain Monte Carlo (MCMC) sampling to obtain best-fit parameters [Foreman-Mackey et al., 2013]. MCMC fits a model to data performing a minimization of residuals. CANNUBI fits tilted ring models created by <sup>3D</sup>BAROLO. The model is convolved with the same resolution as the data. This is essential in order to account for the beam smearing effect of the data. CANNUBI can perform the minimization of the residuals between data and models on either the total flux map (2D) or on the full datacube channel by channel (3D). In this study, the 2D implementation is used, mostly due to time constraints: running CANNUBI on the total flux map for our mock datacubes takes typically 15 hours to achieve convergence with 30 walkers.

MCMC is a widely used method in high dimensional problems aiming to find the parameters that best fit the data of interest. The output of CANNUBI are corner plots that show the marginalised posterior probability distribution for each parameter pair [Foreman-Mackey, 2016]. The parameters have uncertainties of  $1\sigma$ .

### 3.2.2 Parameters in CANNUBI

CANNUBI requires an input file containing both geometrical and kinematic parameters of the galaxy. Given that CANNUBI uses <sup>3D</sup>BAROLO to create galaxy models, several parameters are in common between the two codes. The parameter file holds initial guesses for the parameters to be fitted, it also includes the parameters that are fixed (details below) and the values that set the parameter space for the MCMC sampling. If parameters are not preset in the parameter file, <sup>3D</sup>BAROLO will make an estimate during the fitting process.

The possible free parameters in CANNUBI are the centre of the galaxy disc ( $x_0, y_0$ ), its disc thickness ( $Z_0$ ), the position angle (PA), radial separation of the rings (RADSEP) and the inclination angle (INC). These require initial values and can be set by the user. CANNUBI is designed to estimate at least the centre and inclination simultaneously, while the other three parameters (PA, RADSEP and  $Z_0$ ) can be added to the fit by the user. The tilted ring model requires two parameters to determine the number of rings to be fitted (NRADII) and the spacing between each pair of rings (RADSEP). Since both of these parameters are correlated to the radial extent of the galaxy, CANNUBI only fits RADSEP. Since we want to properly sample the data without

overfitting, we choose the value of `RADSEP` to be approximately the same as the beam of the observation in order to sample resolution independent rings. Petunia has an approximate radial extent of 1.2 kpc ( $0.23''$ ). This gives the possibility for 6 independent rings for the high resolution mocks ( $0.02''$ ) and 3 independent rings for the medium resolution mock ( $0.05''$ ). For the main parameters (`INC`, `PA`, `Z0`), `CANNUBI` determines a single value per galaxy disc, i.e. they are always assumed to be constant with radius.

The initial values for the kinematic parameters are the systematic velocity ( $v_{sys}$ ), rotational velocity  $v_{rot}$ , velocity dispersion  $v_{disp}$  and the radial velocity  $v_{rad}$ . `CANNUBI` will initially perform one kinematic fit with `3D BAROLO` and will maintain this kinematic model fixed during the MCMC sampling of the geometric parameters. If instead the fit with `CANNUBI` is performed on the full datacube, calculating the residuals and performing the minimization must be done per channel map, this is the main reason of the much longer time requirement.

Before the modeling, `3D BAROLO` masks the data and the masking technique can be chosen. In our cases we use the method `SMOOTH&SEARCH`. The data are first smoothed to a lower resolution and then scanned for sources with the task `SEARCH` [Di Teodoro and Fraternali, 2015]. The smoothing parameters are: the factor at which smoothing is performed (`FACTOR`) and the S/N at which the data are cut (`BLANKCUT`). We smooth by a `FACTOR = 2` and cut at `BLANKCUT = 3`. The source scanning parameters are: the primary S/N cut applied (`SNRCUT`) and the secondary S/N used for growing the detected sources (`GROWTHCUT`). We use `SNRCUT = 3` and `GROWTHCUT = 2`. In this way the mask is sufficiently large so that the model is not artificially cut with respect to the data while being small enough that noise and non-target sources are eliminated.

Finally, we need to set the number of walkers and iterations for the MCMC. There is also the option to let the MCMC run up to convergence for the best result. This convergence is determined using the autocorrelation time<sup>2</sup> and it should assure that the walkers have explored the parameter space sufficiently and have reached a stable distribution, if this is not reached within 20000 iterations then `CANNUBI` automatically stops the exploration. MCMC is ran up to convergence for Petunia with an inclination of  $30^\circ$  and  $60^\circ$  and  $80^\circ$  used in all cases.

In appendix A, we report the parameters used in `CANNUBI` for the Petunia mock with an inclination of  $60^\circ$  and resolution of  $0.02''$ .

### 3.2.3 CANNUBI on idealised galaxy models

Prior to the analysis of Petunia, we examine the behaviour of the algorithm for three rather simple mock galaxies with different geometrical properties obtained with `GALMOD` (see Sec. 2.1). The mocks consist of two thin discs and one thick disc (see Tab. 1). In the MCMC sampling we used 60 instead of 30 walkers in one of the models, since this did not make a big difference in the results we are confident that 30 walkers is sufficient for these models.

In Figure 10, we show the `CANNUBI` outputs: the total flux map with overlapping contours at the same level for both the data and the model.

<sup>2</sup>Available at <https://emcee.readthedocs.io/en/stable/tutorials/autocorr/>.

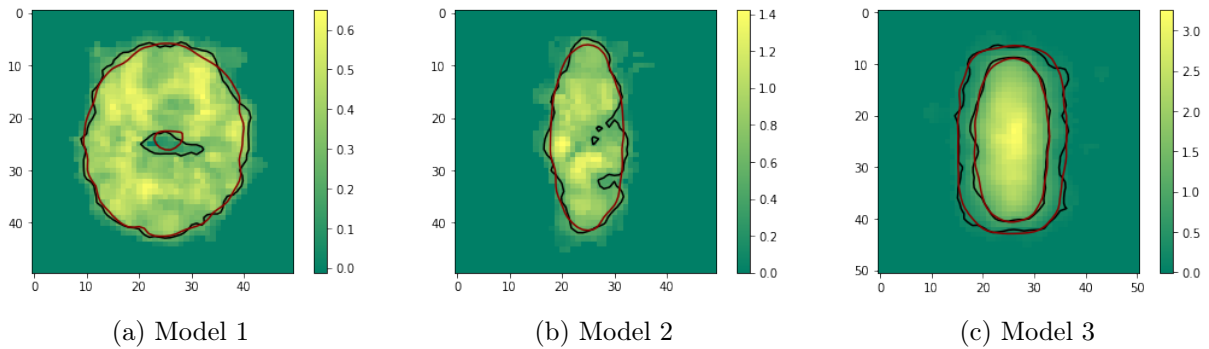


Figure 10: Output of CANNUBI, flux maps of the three idealised models. We show contours at the same levels for the data (in black) and the best-fit model (in red). The color bar is given in  $L_{\odot} \text{kpc}^{-2}$ , while the axes are in pixels (1 pixel  $\approx 20''$ ).

The recovered inclinations are visualized in the left panel of Figure 11, where the true values are shown on the x-axis and the recovered values are shown on the y-axis, the identity line indicates perfect recovery. On the right panel, we show the plot for the disc thickness. In Table 1, the recovered values and their uncertainties are listed.

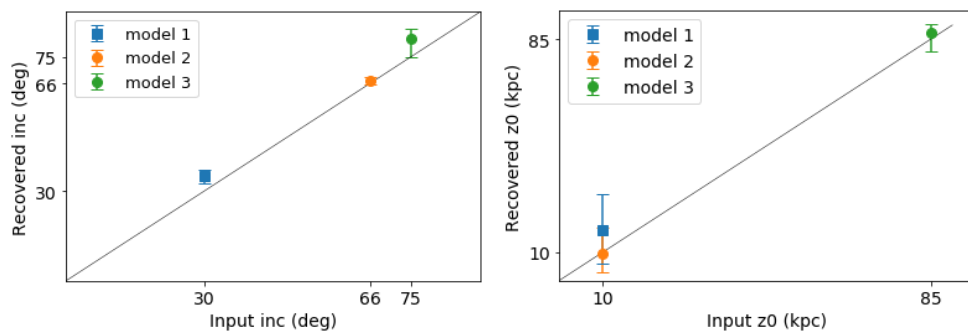


Figure 11: Comparison plot of input and recovered values for inclination (left panel) and thickness (right panel) using CANNUBI. The models are referred to with colored markers. The identity line (in black) represents perfect recovery.

Model	True inc	Recovered inc (deg)	True Z0	Recovered Z0 (arcsec)
1.	30	$35.2^{+2.0}_{-2.5}$	10	$17.7^{+14.0}_{-11.2}$
2.	66	$67.1^{+1.3}_{-1.0}$	10	$9.7^{+9.0}_{-6.7}$
3.	75	$81.2^{+3.0}_{-6.5}$	85	$87.2^{+3.0}_{-6.4}$

Table 1: True and recovered values for the inclination and thickness for the three mock idealised galaxies.

## 4 Results and Discussion

In this Chapter, we present and analyze the findings regarding the thickness and inclination of the simulated galaxy Petunia. First, we examine the obtained value for thickness obtained from the noise-free edge-on view of Petunia. Subsequently, we discuss the outcomes of the geometrical fitting performed using *CANNUBI* on the mock data of Petunia. At last, we will go over the reliability and the implications of this research.

### 4.1 True thickness of Petunia

Multiple thicknesses were determined of the simulated galaxy Petunia from the edge-on view from the vertical light distributions along the full extent of the disc, like the one visualized in Figure 6. The thicknesses obtained are plotted as a function of the radius as can be seen in Figure 12. We find a median thickness of  $0.065^{+0.002}_{-0.009}$  kpc. The green markers represent the right side of the disc in Figure 12 and the orange ones the left side. It is clear that on the right side of the disc there are less data points. These have been left out on purpose, because the  $R^2$  was relatively low (right panel of Fig. 8), this is likely due to the warp seen on the right side of Petunia and the dominant presence of the diffuse emission (Fig. 5).

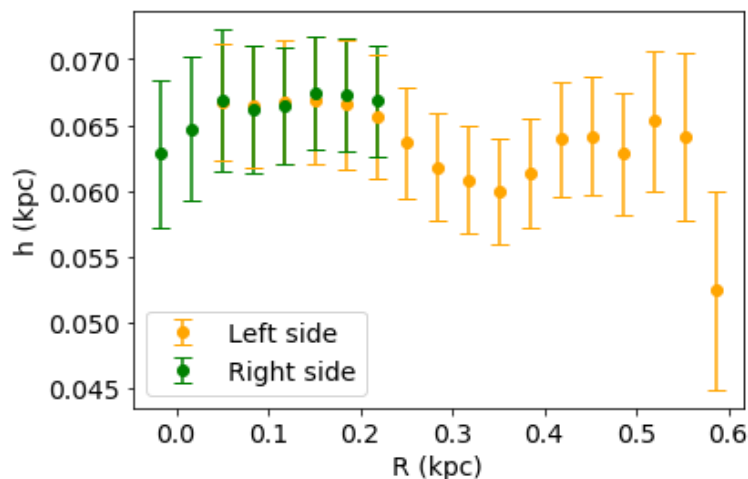


Figure 12: Thicknesses ( $h$ ) obtained from the edge-on profile of Petunia as a function of the radius ( $R$ ) of the disc. The left side (orange) has more data points than the right (green) due to poorly fitted vertical profiles.

We find that the thickness remains approximately constant as a function of radius. Therefore, taking the median value of the  $h$ -distribution is a good description of the global value of the disc thickness. However, we note that the presence of a constant thickness is not observed in real galaxies at low- $z$ , where it is usual for the discs to be flared, i.e. they are thicker in the outskirts than in the central regions (e.g. [Bacchini et al., 2019]). The lack of flaring in Petunia may be caused by two effects: 1. the radial change of thickness is not large enough to be detected; 2. the presence of a warp may be affecting the outskirts of Petunia. The interesting implication is that these simulations being realistic representations of galaxies, perhaps the disc thickness in real high- $z$  galaxies may also not significantly change with radius. Therefore, measuring a single thickness with *CANNUBI*, which assumes a constant value with radius, may be justified.

## 4.2 CANNUBI on the simulated galaxy Petunia

In this Section, we present the main results of this work which consists of the estimation of the inclination and thickness of the disc of the simulated galaxy Petunia. We run CANNUBI on mock datacubes extracted from the SERRA simulation with three different disc inclinations w.r.t the line-of-sight. We use CANNUBI to simultaneously obtain inclination and thickness from these data, as it would be done with real galaxies, and compare the estimates with the true values.

### 4.2.1 Flux maps

As mentioned, CANNUBI outputs the total flux map of the surface brightness obtained from the input datacube and overlays on this the best fit model. We show these outputs in Figure 13 with the data (black contour) and the obtained best-fit model (red contour). The white contour represents the cut-off of the mask that  ${}^3D_{\text{Barolo}}$  has created. The increase in inclination is recognized in the increasing surface brightness on the colorbar and the decreasing size of the minor axis of the galaxy disc.

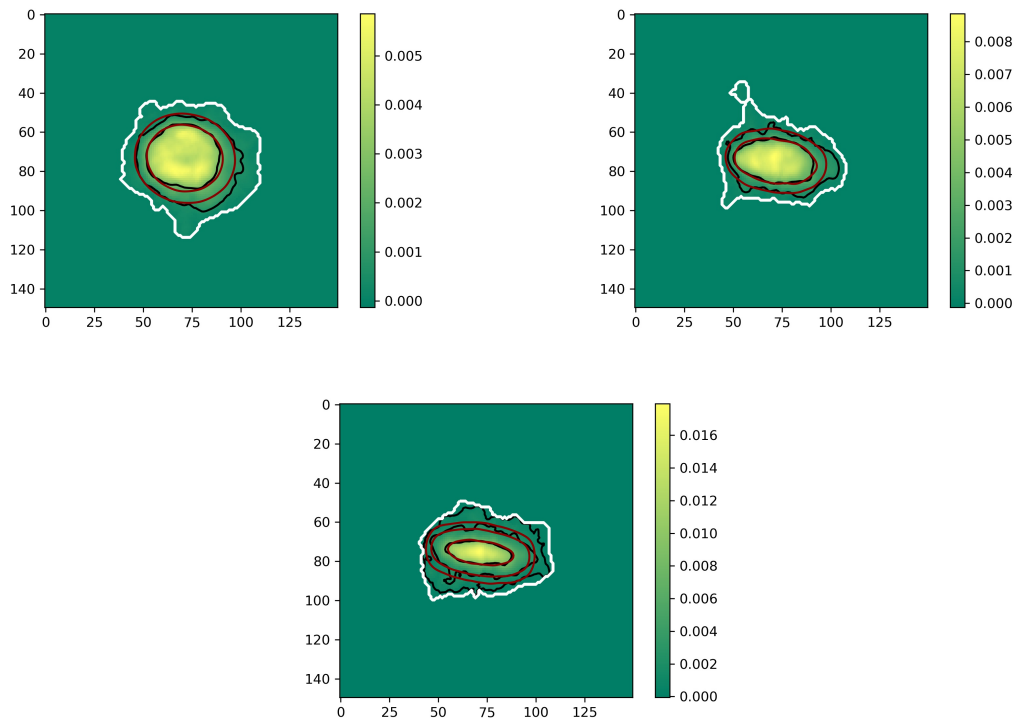


Figure 13: The total surface brightness flux map of Petunia by CANNUBI. The contours of the data are shown in black and those of the best-fit model in red. The colorbar is given in  $L_{\odot}kpc^{-2}$ , while the axes are in pixel (1 pixel  $\approx 0.004$  arcsec). Upper left panel: An inclination of  $30^{\circ}$ . Upper right panel: An inclination of  $60^{\circ}$ . Lower panel: An inclination of  $80^{\circ}$ . The angular resolution of all these mock datacubes is  $0.02''$ .

As we can see from Figure 13, CANNUBI succeeded in fitting the emission-line data quite well. The red contours match the shape of the black contours except for the very outer parts of the mock galaxy at  $80^{\circ}$  inclination. This may be due to the presence in the simulation of significant diffuse emission outside the bright disc as we have seen in Section 2.2. The masks look good in

general, however on the inclination of  $80^\circ$  it is a bit tight possibly for the same reason mentioned previously. Overall, we can conclude that the global distribution of the emitting gas in this simulated galaxy appear to be well reproduced by tilted ring models with  $INC$ ,  $PA$  and  $Z0$  constant with radius.

In order to test the effect of angular resolution on the recovered parameters we also ran CANNUBI on a datacube of Petunia at  $60^\circ$  inclination obtained with angular resolution of  $0.05''$ . The total flux map and its contours are shown in Figure 14. The red contours match the shape of the black contour quite well. The mask captures other emitting sources than the disc but this does not seem to effect the red contours. In comparison to Petunia on an inclination of  $60^\circ$  with an angular resolution of  $0.02''$  the disc seems to be smaller, this is most likely due to the resolution, which contains of  $\sim 2.3$  elements over the radius of the disc. It leads to a smaller maximum brightness, which is visible in the maximum of the colorbar in Figure 14 compared to Figure 13, due to averaging with the less brighter part of the disc. On the outskirts of the disc there is the risk of averaging with the surrounding noise and as a consequence the galaxy appears to be smaller.

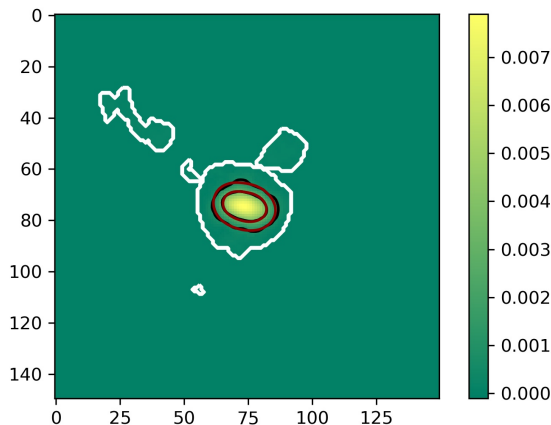


Figure 14: Output of CANNUBI, flux maps of the simulated galaxy Petunia at an inclination of  $60^\circ$  at an angular resolution of  $0.05''$ . The contours of the data are shown in black and those of the best-fit model in red. The colorbar is given in  $L_\odot kpc^{-2}$ , while the axes are in pixels (1 pixel  $\approx 0.004$  arcsec).

#### 4.2.2 Recovered inclination and thickness

In this Section, we show and describe the recovered thickness and inclination of the simulated galaxy Petunia using CANNUBI. Table 2 lists the recovered values, their uncertainties and true values, with Figures 15 and 16 showing the recovery plots.

In Figure 15, we show the inclinations recovered by CANNUBI using the mock datacubes at inclinations  $30^\circ$ ,  $60^\circ$  and  $80^\circ$ . In the plot it is distinguished between the two resolutions:  $0.02''$  and  $0.05''$ . The uncertainties can be seen in the errorbars ( $1\sigma$  of the posterior distribution). The inclinations recovered by CANNUBI are compatible within the errors. The uncertainties for angular resolution of  $0.02''$  are very similar, for  $0.05''$  the uncertainty is significantly larger. This is expected because of less resolution elements. While for the high angular resolution ( $0.02''$ ),

we explored the data using 6 rings in total, for the medium resolution we only used 3 rings. Moreover, the overall shape of the total map is significantly influenced by the resolution and it becomes more difficult to estimate both inclination and thickness.

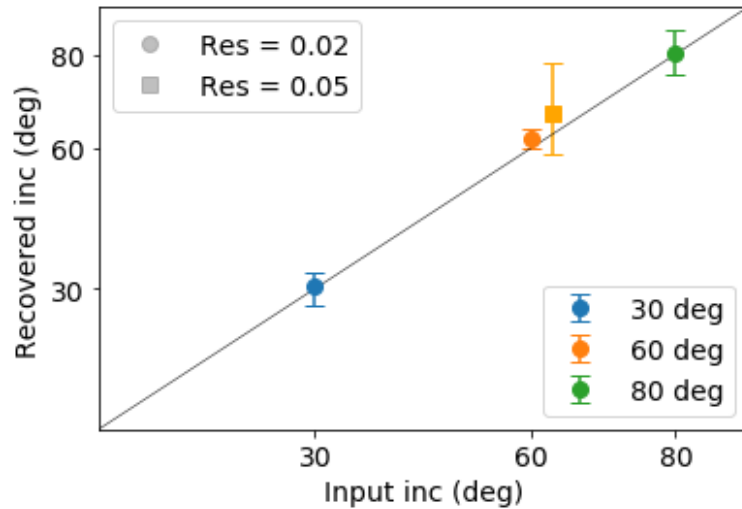


Figure 15: CANNUBI’s recovered inclinations for the Petunia simulated galaxy compared to the input inclinations. The different inclinations are indicated by colors displayed in the lower right legend. The marker distinguishes between the resolution of  $0.02''$  (circle) and  $0.05''$  (square). The identity line (in black) represents perfect recovery. Note that the two points at  $60^\circ$  have been slightly shifted for presentation purposes.

The recovered thicknesses for each inclination of Petunia are shown in Figure 16. The comparison with the true thickness is visualized by plotting its value as a horizontal blue line with its uncertainty range in shaded blue. The inclinations and resolutions are distinguished in the same manner as in Figure 15. The disc thickness recovered by CANNUBI for the inclinations of  $30^\circ$  and  $60^\circ$  are compatible within the errors of the true value. However, the inclination of  $80^\circ$  is slightly overestimated and not compatible within the errors. The uncertainties on the values for an angular resolution of  $0.02''$  are decreasing significantly (factor of  $\sim 2$ ) as the inclinations increases. This behaviour is mostly likely due to the projection becoming less visible for lower inclined discs.

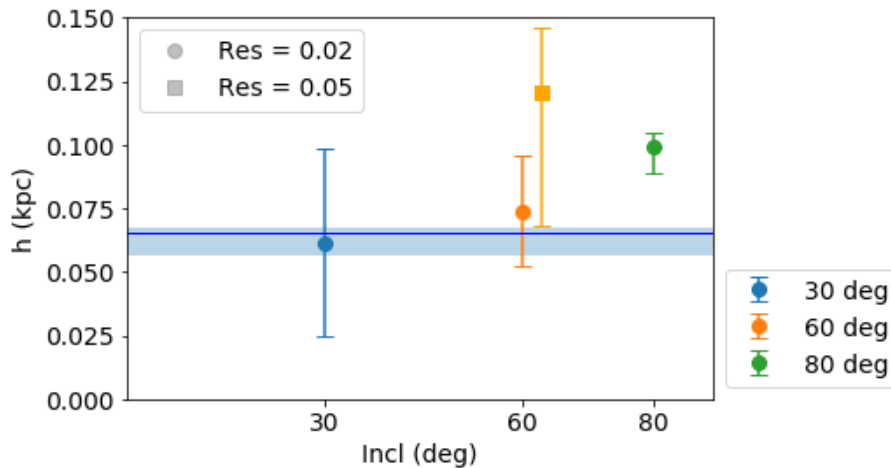


Figure 16: CANNUBI’s recovered thicknesses for Petunia as a function of their inclination. The blue line is the most likely true value of the thickness estimated from the edge-on profile and the shaded region represents its  $1\sigma$  uncertainties. Note that the two points at  $60^\circ$  have been slightly shifted for presentation purposes.

The precise values can be found in Table 2 where we show the true values for inclination, thickness, the recovered values and their uncertainties. In appendix B, we show the corner plots of the fits on the mock galaxies obtained in this study.

True inc (deg)	Resolution (arcsec)	Recovered inc (deg)	Recovered Z0 (kpc)
30	0.02 ( $\sim 0.10kpc$ )	$30.4^{+3.0}_{-4.1}$	$0.06 \pm 0.04$
60	0.02 ( $\sim 0.10kpc$ )	$62.1^{+2.0}_{-2.4}$	$0.07 \pm 0.02$
60	0.05 ( $\sim 0.26kpc$ )	$67.3^{+11.0}_{-8.8}$	$0.12^{+0.03}_{-0.05}$
80	0.02 ( $\sim 0.10kpc$ )	$80.2^{+5.4}_{-4.3}$	$0.10 \pm 0.01$

Table 2: Precise values including errors for the true and recovered inclination, as well as the recovered thickness for the simulated galaxy Petunia. The true thickness is  $0.065^{+0.002}_{-0.009}$  kpc.



### 4.3 Reliability

In Section 4.1, we showed that the thickness of Petunia is radially constant. However as mentioned earlier, the warp and the poor fits in the outskirts may have impacted the recovered values of the thickness. The reliability of the constant trend between radius and scale height could be improved when we have a better indication of the 3D shape of Petunia, which could be achieved by examining different azimuthal projections of the light distribution of Petunia with several edge-on total flux maps.

The disc thickness recovered with CANNUBI for Petunia are 0.06 and 0.07 kpc for the 30° and 60°, respectively. We note that these values are below the angular resolution of the synthetic observations of 0.02'' ( $\sim 0.10$  kpc). This also happens for the medium resolution datacube at 60°, which we recover a thickness of 0.12 kpc and the angular resolution is 0.05'' ( $\sim 0.26$  kpc). This is a promising result, indicating that in spite of the real disc thickness being smaller than the resolution of the data, CANNUBI is still able to consistently and accurately recover in the range of disc thickness and inclinations tested. This suggests that CANNUBI is properly accounting for the convolution.

In Section 3, it is discussed that CANNUBI has the possibility to perform the minimization over all the channels of the datacube (3D) or over the corresponding total flux map (2D). In this study, we used CANNUBI to analyze the total surface brightness flux map. The thickness of the disc affects the total flux map such as the ones shown in Figure 9. This is why it was possible to retrieve information about thickness using the 2D implementation of CANNUBI in [Roman-Oliveira et al. \[2023\]](#). Moreover, in the same work they have attempted to use the 3D implementation of CANNUBI which appeared to be a promising way to break the degeneracy between inclination and thickness even further, however this was not fully tested. For Petunia, the resulting disc thickness seems to be thin in comparison to radial extent, and the 2D implementation worked well. However, for the high inclination case it performed significantly worse due to a stronger degeneracy in the inclination and thickness, as seen in the posterior plot shown in Appendix B. The thickness measurement in that case could benefit from running Petunia in the 3D implementation of CANNUBI. This is very computationally expensive, but could be done in a future project.

### 4.4 Implications

CANNUBI is tested successfully on ALMA synthetic observations of Petunia. These tests support the results on the thickness of  $z = 4.5$  galaxies studied in [Roman-Oliveira et al. \[2023\]](#). In this work, CANNUBI was applied on ALMA observations of five  $z = 4.5$  galaxies, finding values of the thickness of the order of 1 kpc. Considering the degeneracy between inclination and thickness, when the thickness is taken into account the maximum rotational velocity increases by  $\sim 10\%$  [[Roman-Oliveira et al., 2023](#)].

The thickness of the discs reported in [Roman-Oliveira et al. \[2023\]](#) are consistent with the thickness of the thick stellar discs found in the Milky Way and other nearby spiral galaxies. This finding may support the galaxy formation scenario indicating that stellar thick discs form during the early stage of the galaxy from turbulent thick gas discs. However, it is challenging to establish an evolutionary connection between low and high- $z$  discs. This is especially difficult given that the majority of galaxies observed at  $z > 2$  tend to be very massive and often starbursting and therefore they are not direct progenitors of disc galaxies observed in the nearby Universe.

## 5 Conclusions

The objective of this thesis is the measurement of the thickness of high-redshift galaxy discs using spatially-resolved observations of gas emission-lines. To date, there are only a handful of studies that tried to estimate the disc thickness of high- $z$  galaxies. The typical resolutions of current observations make the thickness measurement particularly challenging. The motivation of this study is to test whether a novel tool, **CANNUBI**, recently employed in [Roman-Oliveira et al. \[2023\]](#) on ALMA observations of  $z = 4.5$  galaxies, can be considered reliable in recovering the disc thickness. To validate **CANNUBI**, we tested it on ALMA synthetic observations of Petunia, a simulated galaxy from the SERRA suite. The thickness and inclination are strongly degenerate, therefore we compared the true and recovered values of both parameters fitted simultaneously. We summarise our main results as follows:

- i) We made an estimate of the true value of the thickness of Petunia since this was not known. This estimation was obtained by fitting a Gaussian function to the vertical light profile of the disc of Petunia seen in an edge-on projection without noise. We find that the thickness of the disc of Petunia is roughly constant along its radial extent, with a median thickness, defined as the dispersion of the Gaussian function, of  $0.065^{+0.002}_{-0.009}$  kpc.
- ii) We used **CANNUBI** to find the best-fit values for the geometric parameters of Petunia with four different configurations: high resolution data ( $0.02''$ ) with three inclinations ( $30^\circ$ ,  $60^\circ$ ,  $80^\circ$ ), and medium resolution data ( $0.05''$ ) with a  $60^\circ$  inclination. **CANNUBI** was able to recover the true values for the thickness and inclination of the discs within  $1\sigma$  for all cases, except for the thickness of the  $80^\circ$  inclination mock data, which was slightly overestimated.

We conclude that the test of **CANNUBI** on the ALMA synthetic observations of Petunia were successful. This makes further research with **CANNUBI** on real high- $z$  galaxies promising and supports the reliability of previous results. Measuring the gas thickness in galaxies can help improve the reliability of studies on the kinematics of galaxy discs, as high values of thickness can have an effect on the recovery of the kinematics. Furthermore, potential insights in the formation of thick stellar discs can be obtained with larger samples as we gather more data linking the evolution of high- $z$  galaxy populations to the local Universe galaxies. The results obtained with **CANNUBI** and reported in this thesis can still potentially be improved by fitting the galaxies in the full datacube, whereas only the total flux map has been used here. This could help further breaking the degeneracy between disc inclination and thickness that, in our experiments with simulated galaxy Petunia, we see being quite prominent especially at the high inclination mock of Petunia.

## References

- C. Bacchini, F. Fraternali, G. Pezzulli, A. Marasco, G. Iorio, and C. Nipoti. The volumetric star formation law in the Milky Way. , 632:A127, Dec. 2019. doi: 10.1051/0004-6361/201936559.
- C. Bacchini, F. Fraternali, G. Pezzulli, and A. Marasco. The volumetric star formation law for nearby galaxies. Extension to dwarf galaxies and low-density regions. , 644:A125, Dec. 2020. doi: 10.1051/0004-6361/202038962.
- A. Bosma. *The distribution and kinematics of neutral hydrogen in spiral galaxies of various morphological types*. PhD thesis, University of Groningen, Netherlands, Mar. 1978.
- C. L. Carilli and F. Walter. Cool Gas in High-Redshift Galaxies. , 51(1):105–161, Aug. 2013. doi: 10.1146/annurev-astro-082812-140953.
- E. M. Di Teodoro and F. Fraternali.  $3D$  BAROLO: a new 3D algorithm to derive rotation curves of galaxies. *MNRAS*, 451(3):3021–3033, Aug. 2015. doi: 10.1093/mnras/stv1213.
- S. M. Fall and G. Efstathiou. Formation and rotation of disc galaxies with haloes. *MNRAS*, 193: 189–206, Oct. 1980. doi: 10.1093/mnras/193.2.189.
- D. Foreman-Mackey. corner.py: Scatterplot matrices in Python. *The Journal of Open Source Software*, 1:24, June 2016. doi: 10.21105/joss.00024.
- D. Foreman-Mackey, D. W. Hogg, D. Lang, and J. Goodman. ttemcee/tt: The MCMC hammer. *Publications of the Astronomical Society of the Pacific*, 125(925):306–312, mar 2013. doi: 10.1086/670067. URL <https://doi.org/10.1086%2F670067>.
- M. Kohandel, A. Pallottini, A. Ferrara, S. Carniani, S. Gallerani, L. Vallini, A. Zanella, and C. Behrens. Velocity dispersion in the interstellar medium of early galaxies. *MNRAS*, 499(1): 1250–1265, Nov. 2020. doi: 10.1093/mnras/staa2792.
- J. Kormendy and R. Bender. Structural Analogs of the Milky Way Galaxy: Stellar Populations in the Boxy Bulges of NGC 4565 and NGC 5746. *ApJ*, 872(1):106, Feb. 2019. doi: 10.3847/1538-4357/aafdf.
- H. Koyama and E. C. Ostriker. Pressure Relations and Vertical Equilibrium in the Turbulent, Multiphase Interstellar Medium. *ApJ*, 693(2):1346–1359, Mar. 2009. doi: 10.1088/0004-637X/693/2/1346.
- M. R. Krumholz, B. Burkhardt, J. C. Forbes, and R. M. Crocker. A unified model for galactic discs: star formation, turbulence driving, and mass transport. *MNRAS*, 477(2):2716–2740, June 2018. doi: 10.1093/mnras/sty852.
- K. Kuijken and G. Gilmore. The mass distribution in the galactic disc. I - A technique to determine the integral surface mass density of the disc near the sun. *MNRAS*, 239:571–603, Aug. 1989. doi: 10.1093/mnras/239.2.571.
- P. E. Mancera Piña, F. Fraternali, T. Oosterloo, E. A. K. Adams, E. di Teodoro, C. Bacchini, and G. Iorio. The impact of gas disc flaring on rotation curve decomposition and revisiting baryonic and dark-matter relations for nearby galaxies. *arXiv e-prints*, art. arXiv:2205.12977, May 2022. doi: 10.48550/arXiv.2205.12977.

- A. Pallottini, A. Ferrara, S. Gallerani, C. Behrens, M. Kohandel, S. Carniani, L. Vallini, S. Salvadori, V. Gelli, L. Sommovigo, V. D’Odorico, F. Di Mascia, and E. Pizzati. A survey of high- $z$  galaxies: SERRA simulations. *MNRAS*, 513(4):5621–5641, July 2022. doi: 10.1093/mnras/stac1281.
- Planck Collaboration. iplanck/i2018 results. *Astronomy & Astrophysics*, 641:A6, sep 2020. doi: 10.1051/0004-6361/201833910. URL <https://doi.org/10.1051/0004-6361/201833910>.
- F. Rizzo, S. Vegetti, D. Powell, F. Fraternali, J. P. McKean, H. R. Stacey, and S. D. M. White. A dynamically cold disk galaxy in the early Universe. , 584(7820):201–204, Aug. 2020. doi: 10.1038/s41586-020-2572-6.
- F. Rizzo, M. Kohandel, A. Pallottini, A. Zanella, A. Ferrara, L. Vallini, and S. Toft. Dynamical characterization of galaxies up to  $z \sim 7$ . , 667:A5, Nov. 2022. doi: 10.1051/0004-6361/202243582.
- B. E. Robertson, S. Tacchella, B. D. Johnson, R. Hausen, A. B. Alabi, K. Boyett, A. J. Bunker, S. Carniani, E. Egami, D. J. Eisenstein, K. N. Hainline, J. M. Helton, Z. Ji, N. Kumari, J. Lyu, R. Maiolino, E. J. Nelson, M. J. Rieke, I. Shivaee, F. Sun, H. Übler, C. C. Williams, C. N. A. Willmer, and J. Witstok. Morpheus Reveals Distant Disk Galaxy Morphologies with JWST: The First AI/ML Analysis of JWST Images. *ApJL*, 942(2):L42, Jan. 2023. doi: 10.3847/2041-8213/aca086.
- F. Roman-Oliveira, F. Fraternali, and F. Rizzo. Regular rotation and low turbulence in a diverse sample of  $z$  4.5 galaxies observed with ALMA. *MNRAS*, 521(1):1045–1065, May 2023. doi: 10.1093/mnras/stad530.
- A. J. Romanowsky and S. M. Fall. Angular Momentum and Galaxy Formation Revisited. *ApJS*, 203(2):17, Dec. 2012. doi: 10.1088/0067-0049/203/2/17.
- L. S. Sparke and J. S. Gallagher, III. *Galaxies in the Universe: An Introduction*. Cambridge University Press, 2 edition, 2007. doi: 10.1017/CBO9780511807237.
- P. van der Kruit and K. Freeman. Galaxy disks. *Annual Review of Astronomy and Astrophysics*, 49(1):301–371, 2011. doi: 10.1146/annurev-astro-083109-153241. URL <https://doi.org/10.1146/annurev-astro-083109-153241>.
- P. C. van der Kruit and L. Searle. Surface photometry of edge-on spiral galaxies. I - A model for the three-dimensional distribution of light in galactic disks. , 95:105–115, Feb. 1981.
- P. Virtanen, R. Gommers, T. E. Oliphant, M. Haberland, T. Reddy, D. Cournapeau, E. Burovski, P. Peterson, W. Weckesser, J. Bright, S. J. van der Walt, M. Brett, J. Wilson, K. J. Millman, N. Mayorov, A. R. J. Nelson, E. Jones, R. Kern, E. Larson, C. J. Carey, Í. Polat, Y. Feng, E. W. Moore, J. VanderPlas, D. Laxalde, J. Perktold, R. Cimrman, I. Henriksen, E. A. Quintero, C. R. Harris, A. M. Archibald, A. H. Ribeiro, F. Pedregosa, P. van Mulbregt, and SciPy 1.0 Contributors. SciPy 1.0: Fundamental Algorithms for Scientific Computing in Python. *Nature Methods*, 17:261–272, 2020. doi: 10.1038/s41592-019-0686-2.
- F. Walter, M. Neeleman, R. Decarli, B. Venemans, R. Meyer, A. Weiss, E. Bañados, S. E. I. Bosman, C. Carilli, X. Fan, D. Riechers, H.-W. Rix, and T. A. Thompson. ALMA 200 pc Imaging of a  $z$  7 Quasar Reveals a Compact, Disk-like Host Galaxy. *ApJ*, 927(1):21, Mar. 2022. doi: 10.3847/1538-4357/ac49e8.

- B. J. Weiner, C. N. A. Willmer, S. M. Faber, J. Melbourne, S. A. Kassin, A. C. Phillips, J. Harker, A. J. Metevier, N. P. Vogt, and D. C. Koo. A Survey of Galaxy Kinematics to  $z \sim 1$  in the TKRS/GOODS-N Field. I. Rotation and Dispersion Properties. *ApJ*, 653(2):1027–1048, Dec. 2006. doi: 10.1086/508921.
- P. Yoachim and J. J. Dalcanton. Structural Parameters of Thin and Thick Disks in Edge-on Disk Galaxies. , 131(1):226–249, Jan. 2006. doi: 10.1086/497970.
- D. G. York and et al. The Sloan Digital Sky Survey: Technical Summary. *The Astronomical Journal*, 120:1579–1587, September 2000. doi: 10.1086/301513.

## Appendix A

Key	Value
nradii	6
radsep	0.019
xpos	148
ypos	148
vrot	200
vrad	0
vdisp	20
inc	30
z0	0.0
norm	azim
pa	90
distance	1078
free	vrot vdisp
linear	0.42
mask	smooth&search
factor	2
blankcut	3
snrcut	3
growthcut	2
noise	9.7e-5
runmcmc	convergence
inclmin	15
inclmax	85
radsepmin	0.6
radsepmax	1.4
z0min	0
z0max	5
nwalkers	30
runs	1000

Table 3: The parameter file that **CANNUBI** requires for Petunia at an inclination of  $60^\circ$  and resolution of  $0.02''$ . In this Table the parameters relevant to this thesis are shown, this includes: the initial values, the free parameters, the options for the mask, the noise, the options for MCMC and the values for the parameter space.

## Appendix B

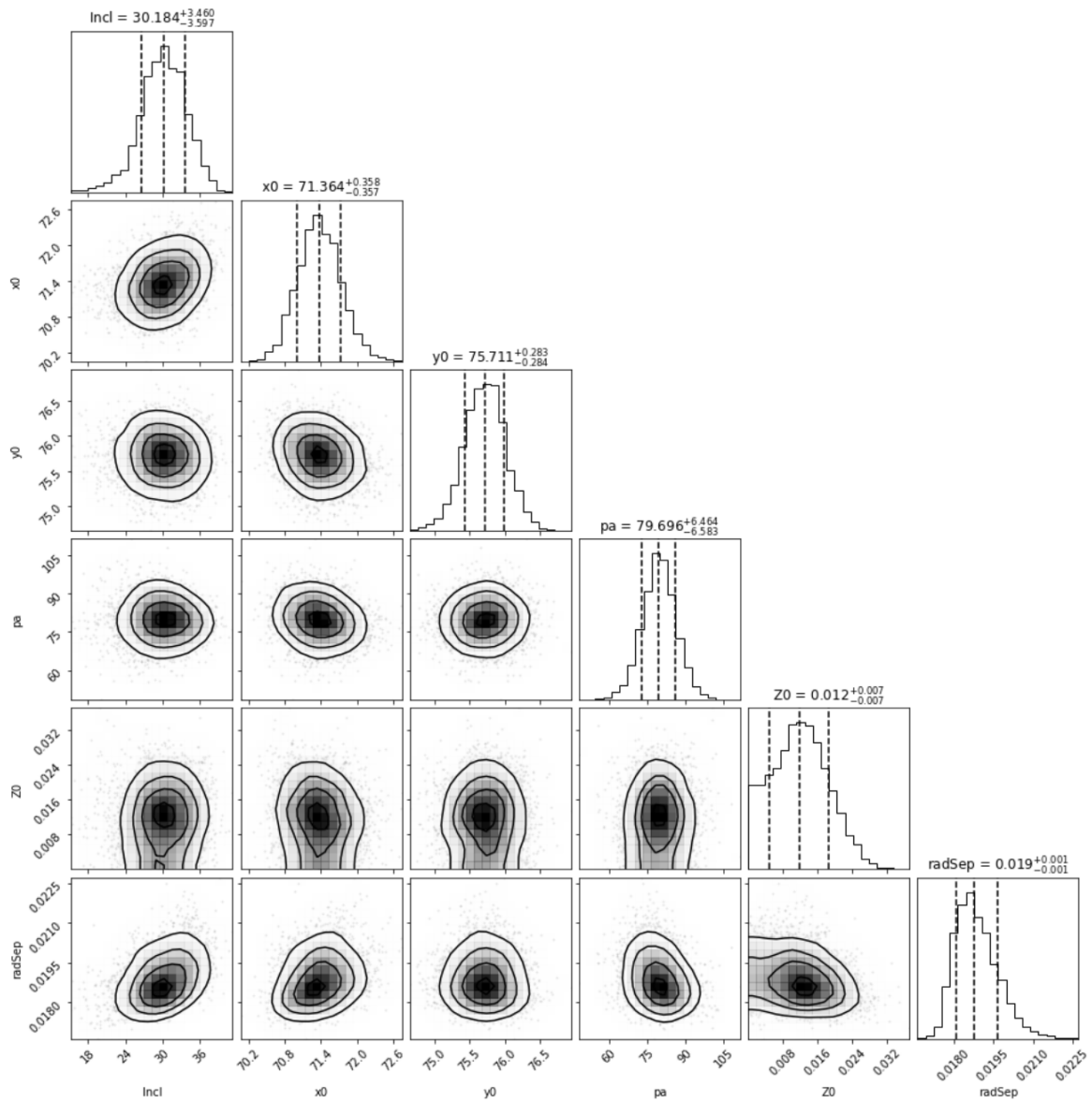


Figure 17: Posterior distributions on Petunia at an inclination of  $30^\circ$  and an angular resolution of  $0.02''$ . From left to right, the INC (deg),  $x_0$  &  $y_0$  (pixel), PA (deg),  $Z_0$  (arcsec) and RADSEP (arcsec) are shown. The inner dashed line represents the mean of the marginalized posterior distribution and the outer dashed lines its  $1\sigma$  errors.

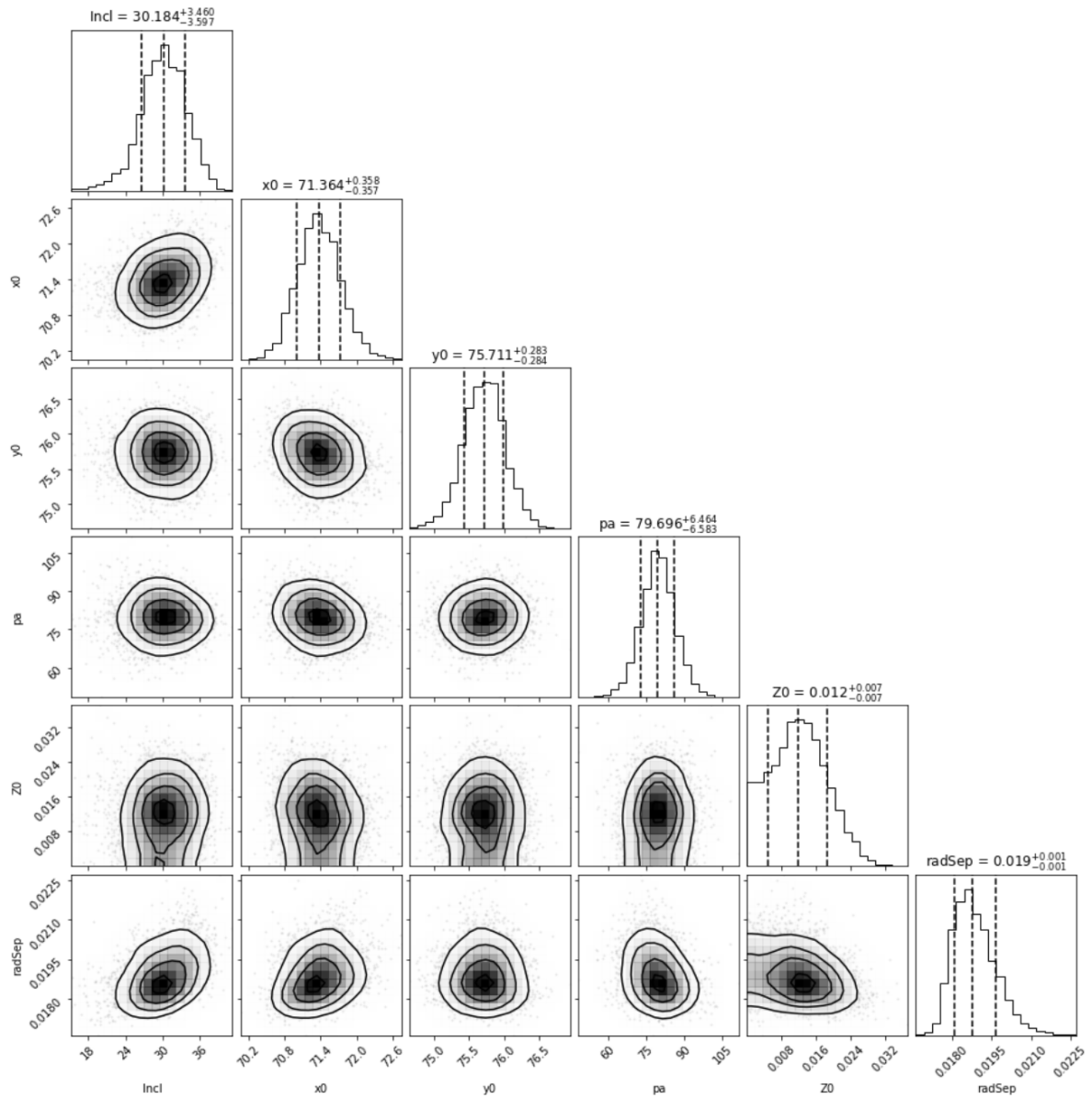


Figure 18: Posterior distributions on Petunia at an inclination of  $60^\circ$  and an angular resolution of  $0.02''$ . From left to right, the INC (deg),  $x_0$  &  $y_0$  (pixel), PA (deg), Z0 (arcsec) and RADSEP (arcsec) are shown. The inner dashed line represents the mean of the marginalized posterior distribution and the outer dashed lines its  $1\sigma$  errors.



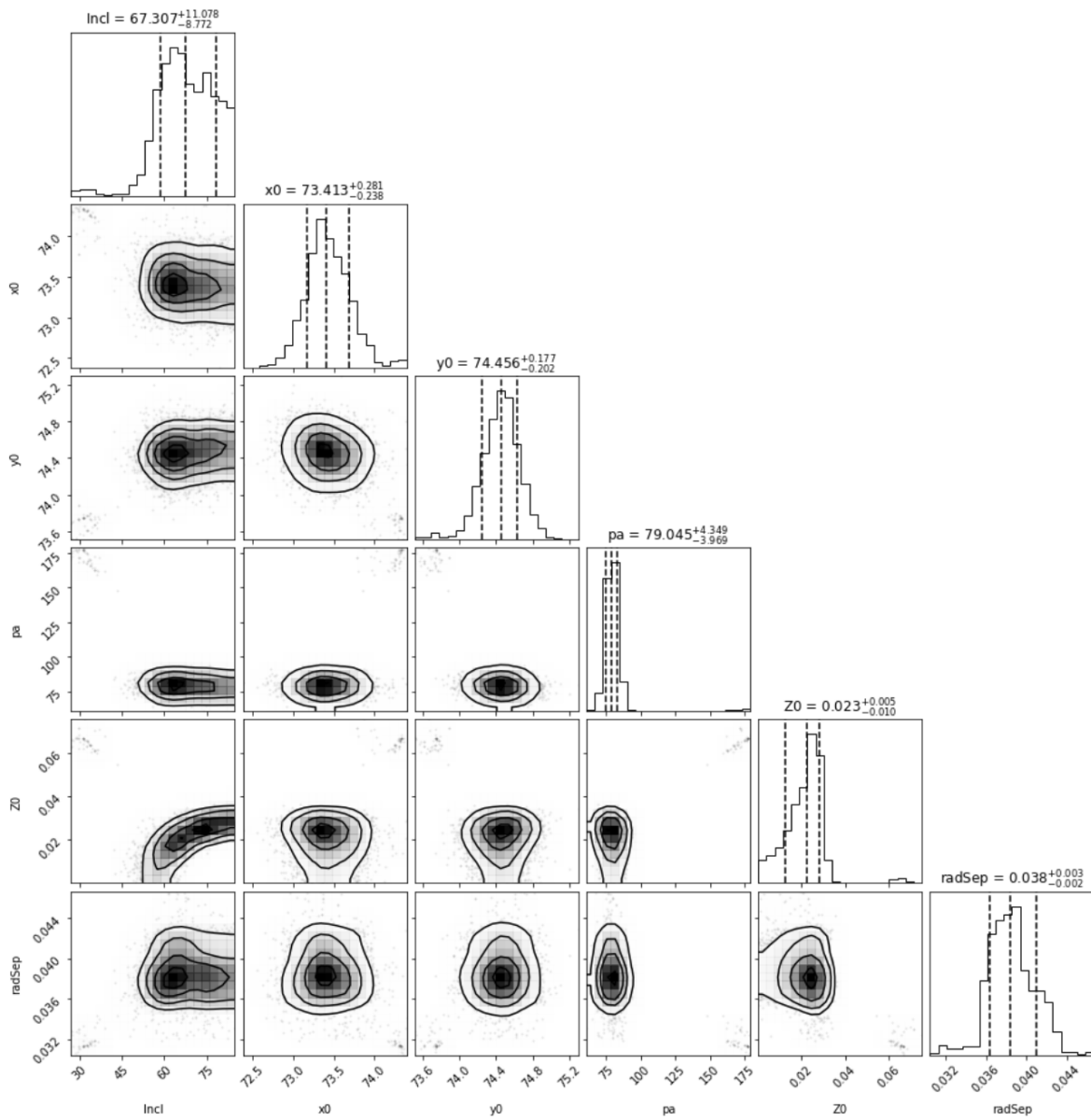


Figure 19: Posterior distributions on Petunia at an inclination of  $60^\circ$  and an angular resolution of  $0.05''$ . From left to right, the INC (deg),  $x_0$  &  $y_0$  (pixel), PA (deg),  $Z_0$  (arcsec) and RADSEP (arcsec) are shown. The inner dashed line represents the mean of the marginalized posterior distribution and the outer dashed lines its  $1\sigma$  errors.

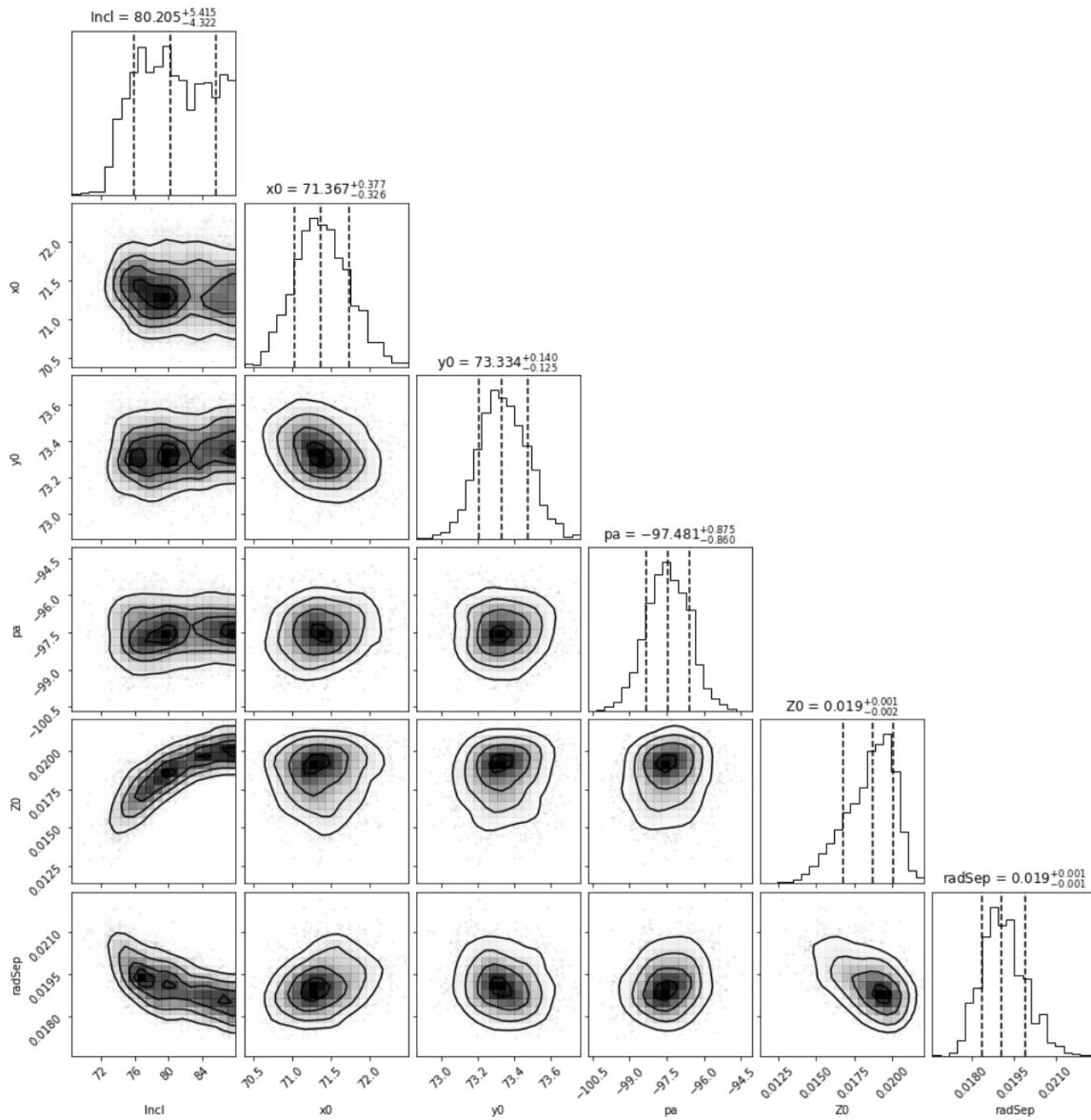


Figure 20: Posterior distributions on Petunia at an inclination of  $80^\circ$  and an angular resolution of  $0.02''$ . From left to right, the INC (deg),  $x_0$  &  $y_0$  (pixel), PA (deg),  $Z_0$  (arcsec) and RADSEP (arcsec) are shown. The inner dashed line represents the mean of the marginalized posterior distribution and the outer dashed lines its  $1\sigma$  errors.